

## A code to simulate neutral beams across TJ-II for the exploitation of a charge-exchange recombination spectroscopy diagnostic

J.M. Carmona, K. J. McCarthy, R. Balbín, J. M. Fontdecaba, J. Guasp, I. Pastor, J. Herranz  
*Laboratorio Nacional de Fusión, Asociación EURATOM-CIEMAT, E-28040 Madrid, Spain*

### Introduction

The TJ-II is a 4-period, low magnetic shear, stellarator device with average minor radius  $\leq 0.22$  m and major radius of 1.5 m whose magnetic configurations are created by a system of external field coils. It is designed to explore a wide range of rotational transforms ( $0.9 \leq t(0)/2\pi \leq 2.2$ ) in low shear configurations ( $\Delta q/q < 6\%$  in vacuum). To date, central electron densities and temperatures up to  $1.7 \times 10^{19} \text{ m}^{-3}$  and 2 keV respectively have been achieved in plasmas created and maintained by electron cyclotron resonance heating ( $f=53.2$  GHz tuned to 2nd harmonic,  $P_{\text{ECRH}} \leq 600$  kW, X-mode polarization). Recently, operation has commenced on one of two neutral beam injectors (NBI) each of which will produce  $\leq 300$  ms pulses of neutral hydrogen accelerated to  $\leq 40$  keV to provide up to 1.2 MW of additional heating.

A diagnostic neutral beam injector (DNBI) is being installed in TJ-II to provide spatially resolved

charge-exchange recombination spectroscopy (CXRS) and neutral particle analysis (NPA) measurements [1]. It is an upgraded version of the compact DINA-5 injector installed on the Madison Symmetric Torus device. It consists of a cold-cathode arc-discharge plasma generator, a four-electrode multi-aperture ion optical system for beam focusing and an ion neutralization duct [2]. Additional features include the possibility to vary the vertical angle of the beam penetration into the plasma by  $\pm 3^\circ$  (by  $\pm 5$  cm at the plasma centre) in order that the beam traverses the magnetic axis for all configurations.

A code has been developed to simulate the neutral beam and its interaction in TJ-II plasmas with the goal of obtaining density profiles of fully stripped ions by comparison between measured and simulated CXRS profiles. This code takes account of parameters such as focal length, divergence and total extracted current,  $T_e$  and  $N_e$  profiles [3], as well as TJ-II magnetic configuration when predicting the beam shape evolution and attenuation as well as

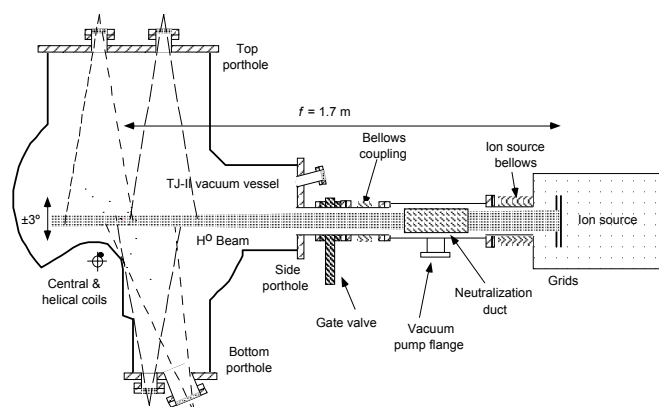


Fig. 1: Cross-sectional view of the TJ-II vacuum chamber and the DNBI.

spectral line emissivity. It also considers light collection and losses as well as spectrograph and detector efficiencies in the dedicated CXRS spectroscopy system [2].

### Code Description

The main DNBI parameters are its 30 keV energy, 170 cm focal length, 5 ms pulse length, and 4 A extracted ion current (where  $H_1^+ \approx 90\%$ ,  $H_2^+ \approx 8\%$ ,  $H_3^+ \approx 2\%$ ). In its current form the code takes account of beam neutralisation, evolution, attenuation and resultant spectral line emissivity as well as light collection. Plume and halo effects are not included as these are minimum for heavy impurities and for C VI ( $n=8 \rightarrow 7$ ) transitions excited by a 30 keV beam.

**Beam components:** Once the singly charged components traverse the neutralization chamber (they dissociate before being neutralised with 77%, 87% and 88% efficiency respectively), the resultant beam current fractions are  $1 \times 0.9 \times 0.77 + 2 \times 0.08 \times 0.87 + 3 \times 0.02 \times 0.88 = 0.84$  where 64.8% of the beam neutrals have full energy (E), 13.92% have E/2 and 5.28% have E/3. For 4 A of extracted ion current, the equivalent neutral currents are 2.54 A, 0.55 A and 0.207 A for E, E/2 and E/3 respectively, thereby giving a total equivalent neutral current of  $\sim 3.3$  equ. A. Note that beam attenuation due to losses in the vacuum port *etc.*, are considered to be null.

**Beam characterisation:** Now, making some reasonable assumptions about the beam and plasma, beam attenuation and current density can be determined. Since the equivalent current of each component is known ( $I$ ), the *in-vacuum* current density profile at a distance  $z$  from the source and radius  $r$  from the beam centre can be given by [4]

$$j(z,r) = j(z,0) \exp\left(-\frac{\pi}{I} j(z,0) r^2\right) \quad (1)$$

$$j(z,0) = \frac{I}{\pi a^2} \frac{z^{*2}}{z^2} \left(1 - \exp\left(-\frac{\alpha a^2}{z^{*2}}\right)\right) \quad (2)$$

Here  $z_{foc}$  is focal length,  $a$  is grid radius,  $\alpha = (\tan(div))^2$  where  $div$  is beam divergence, and  $z^* = \left(1/z - 1/z_{foc}\right)^{-1}$ . Next, to determine the beam current density at any distance  $z$ , an attenuation coefficient ( $\lambda$ ) that considers the various collisional processes is included. Thus

$$I(z) = I(z_0) \exp\left(-\int_{z_0}^z \lambda dz\right) \quad \text{where} \quad \lambda = n_e \frac{\langle \sigma_e v_e \rangle}{v_b} + n_p \sigma_p^{tot} + n_{imp} \sigma_{imp}^{tot} \quad (3)$$

where  $\sigma_p^{tot}$  and  $\sigma_{imp}^{tot}$  are total cross-sections (ionization plus CX) for protons ( $p$ ) and impurities ( $imp$ ), and  $\langle \sigma_e v_e \rangle$  is the collisional rate coefficient for impact ionisation. The proton ( $N_p$ ) and impurity ( $N_{imp}$ ) densities are obtained from quasi-neutral equations (it is assumed that TJ-II plasmas can be approximated by a single impurity of charge number  $Z$ ).

**Relative velocities and temperatures:** In databases such as ADAS, coefficients are provided as a function of  $T_e$ , as it is considered that  $v_{\text{neutral}} \ll v_{\text{electron}}$ . Since the neutrals here are injected at 30 keV a small correction is made. Hence relative velocities and effective temperatures are defined as ( $e$  and  $b$  indicate electronic and beam):

$$v_r = |\bar{v}_e - \bar{v}_b| = \sqrt{\frac{2E_e}{m_e}} + \sqrt{\frac{3T_e}{M_b}} = v_e \left[ 1 + \delta \sqrt{\frac{E_b}{T_e}} \right] \quad \text{with} \quad \delta = \sqrt{\frac{2m_e}{3M_b}} \quad (4)$$

Since  $E_{\text{eff}} = 1/2 \mu v_r^2 = 3/2 T_{\text{eff}}$  thus  $T_{\text{eff}} = T_e \left[ 1 + \delta \sqrt{E_b/T_e} \right]^2$ .

**Photon collection and detection:** The code also considers spectral line emissivity (for the CVI 529 nm line) as well as the photons collected and detected ( $P_\lambda^{CX}$ ) by the spectroscopy system and CCD camera mounted on a spectrograph. Here, emissivity is a function of local impurity and neutral densities, interaction cross-sections, and branching ratios  $A_{ij}$ , while light collection is a function of solid angle,  $\Delta\Omega$ , pulse length,  $\Delta t$ , as well as component (window, lenses, fibres, couplers, spectrograph, CCD) transmission and efficiencies ( $\chi^{sist}$ ) [5]. Hence

$$P_\lambda^{CX} = \frac{1}{4\pi} \frac{A_{ij(8 \rightarrow 7)}}{\sum A_{ij}} \left( \sum_i \langle \sigma v \rangle_i \int N_i dl \right) N_{\text{imp}} \cdot \Delta\Omega \cdot \Delta t \cdot \chi^{sist} \quad (5)$$

## Simulation Results

As a demonstration of the code, plots of current density ( $\text{A cm}^{-2}$ ) at the beam centre for *in-vacuum* as well as a range of plasma conditions for the standard configuration are shown in Fig. 2. Next, equivalent current density profiles at the plasma centre are plotted for  $N_e(0) = 2 \times 10^{13} \text{ cm}^{-3}$  in Fig. 3. Note; local neutral densities (which are needed to calculate photon fluxes) are obtained by integrating local spectral line emissivities along such profiles as optical lines-of-sight are perpendicular to the beam [2].

Finally, plots of the number of photons detected in each of 12 light collection channels of the CCD are shown in Fig. 4 for the same plasma conditions as in Fig. 2 and for a range of plasma magnetic configurations having  $T_e(0) = 400 \text{ eV}$  and  $N_e(0) = 2 \times 10^{13} \text{ cm}^{-3}$ . The high-count rates given in this Fig. 4 are due to the high throughput of the selected spectrograph, (an f/1.8 Holospec by Kaiser Optical Systems equipped with a high dispersion transmitting

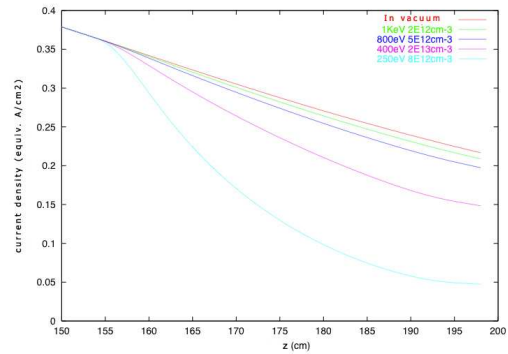


Fig. 2: Equivalent current density ( $\text{A cm}^{-2}$ ) at beam centre vs. distance from DNBI ion source for several plasma conditions ( $T_e(0)$  &  $N_e(0)$  shown). The plasma centre is at 170 cm.

grating [2]) as well as the high efficiencies of the other components selected. In all cases the CCD signal integration time is 5 ms and background as well as passive light signals are not considered here (as these are unknown at present). Also, the high light levels predicted will permit accurate impurity ion velocity and temperature measurements to be made, *i.e.* large numbers of photons ( $\sim 10^4$ ) are needed for CXRS velocity measurements to better than  $1 \text{ km s}^{-1}$ . Also, the use of bi-directional lines-of-sight (see Fig. 1) will aid locating the non-Doppler shifted wavelength position.

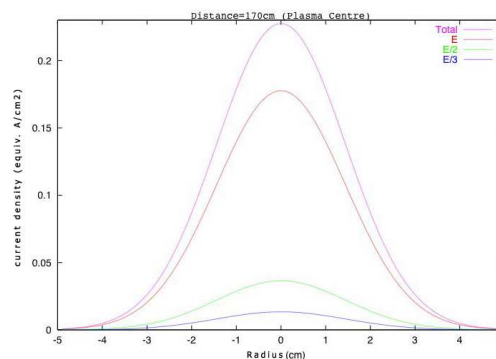


Fig. 3: Equivalent beam neutral current density profiles at distance  $z = 170 \text{ cm}$  from source (at plasma centre) for total and E, E/2, E/3 components when  $\text{Ne}(0) = 2 \times 10^{13} \text{ cm}^{-3}$ . The  $1/e$  radius of the beam is  $\sim 21 \text{ mm}$  at focus.

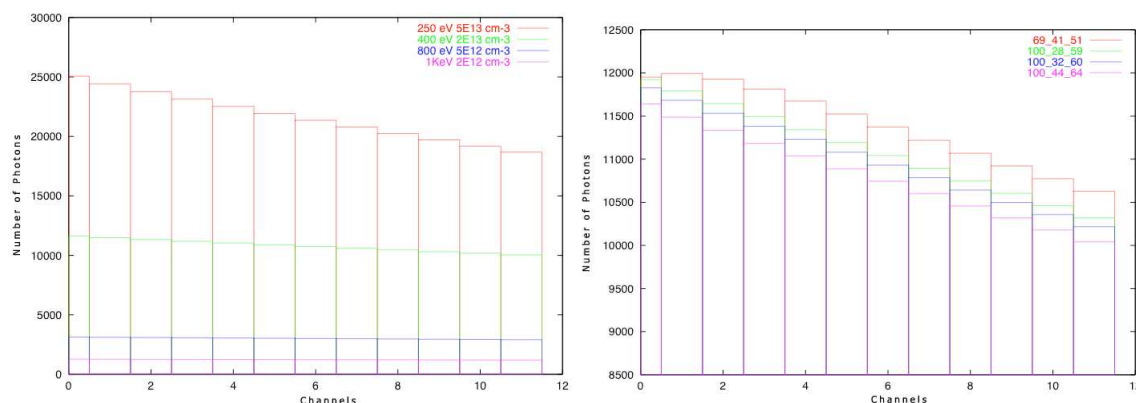


Fig. 4. Predictions of detected photons as a function of CXRS observation channel for a range of plasma conditions in the TJ-II standard configuration (100\_44\_64) and for several TJ-II magnetic configurations [3]. The separation at the beam between the lines-of-sight of channels 1 and 12 is  $\sim 12 \text{ cm}$ . Channel 1 is closest to the DNBI.

## Future work

System installation is almost completed and it is expected begin exploitation in the near future. Once the optical system is absolutely calibrated CXRS data can be analysed by this code thereby providing a tool for determining local C VI densities.

## Acknowledgements

This work is partially financed by the Spanish Ministerio de Educación y Ciencia, Ref. ENE2004-04319/FTN.

## References

- [1] K. J. McCarthy *et al.*, Report No. 1022, CIEMAT, Madrid 2003
- [2] K. J. McCarthy *et al.*, Rev. Sci. Instrum. 75 (2004) 3499
- [3] V. Tribaldos *et al.*, Report No. 963, CIEMAT, Madrid 2001
- [4] J. Mlynar, Report LRP 692/01, CRPP EPFL, Lausanne 2001
- [5] R. J. Fonck *et al.*, Phys. Rev. A 29, 3288 (1984)